Visual Servoing with Quick Eye-Vergence to Enhance Trackability and Stability

Fujia Yu, Wei Song and Mamoru Minami

Abstract— **Visual servoing methods for hand-eye configuration having been presented so far seems to be vulnerable to stable tracking of moving target, leading to disconnection of feedback and dangerous motion of the manipulator being out of control. Our proposal to solve this problem is that the controller for visual servoing of the hand and the one for eye-vergence should be seperated independantly based on decoupling each other and to set relatively high gain to the eye-vergence controller to put the priority to the 3D pose tracking ability (trackability). Proposed method includes two loops: a loop for conventional visual servoing that direct a manipulator toward a target object and an inner loop for active motion of binocular camera for accurate and broad observation of the target object. The effectiveness of the hand & eye-vergence visual servoing is evaluated through simulations incorporated with actual dynamics of 7-DoF robot with additional 3-DoF for eye-vergence mechanism of left and right camera's motion, on the view points of how the new idea improved the stability and trackability against quick motion of the target.**

I. Introduction

Tasks in which visual information are used to direct a manipulator toward a target object are referred to visual servoing in [1], [2].

However, most visual servoing researches focus attention on robot control problem, and simplify or omit the object measurement problem, which is thought to be dealt with in another research field: robot vision field. The point is that we have to enhance both the camera observability and the robot stability simultaneously, because they affect each other in visual servoing. Keeping suitable viewpoint is important for object observation. It can provide more information of the object for fast and correct recognition. Some methods are proposed to improve observability of the object. However, these methods only increase the number of cameras to give different views to observe the object, the cameras in these systems lack the adaptability to a changing environment, that is, the ability to change the viewpoint along with the moving object, and tracking it. So in visual servoing application it is important to make the object in the visual field of the camera. Also for the mass of the manipulator is much more than the camera, when the view point of the camera have to change very fast (for example when the object moves quickly), the manipulator may not satisfy the request, in this case, because of the small mass and moment inertia of the camera, we can change the viewpoint faster and track the object better. Since the cameras and the end-effector do different tasks - camera is used for observe the target object, and the end-effector is to move toward the target object - it is reasonable to separate the motion of the camera and the motion of the end-effector. In this paper, we present a hand & eye-vergence dual visual servoing system as shown in Fig. 1, in which the hand-visual servoing loop includes the active motion of binocular camera to maximize accurate and broad observation of the target object.

Fujia Yu, Wei Song and Mamoru Minami are with Department of Human and Artificial Intelligence Systems, Graduate School of Engineering, University of Fukui, Fukui, 910–8507, Japan { yufujia, songwei, minami } @rc.his.fukui-u.ac.jp

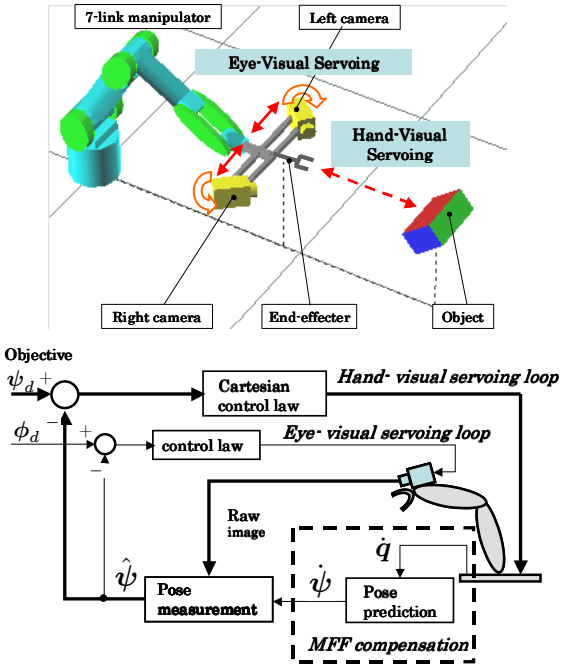

Fig. 1. Hand & Eye Visual servo system

With an eye-in-hand configuration, a problem exists, that is the motion of the end-effector cause a fictional motion of the object. Consider about the human's action, we can perceive the target pose in the world coordinate by subtracting the fictional motion caused by the motion of ourselves, thus the influence on recognition from the ego motion can be compensated. To realize this compensation of ego motion, it is better to use the kinematics relation of robot to calculate the fictional motion, thus we chose position-based method instead of image-based method. To apply such a intelligence into recognition system, we propose an robust recognition method, called motion-feedforward (MFF) compensation method. The MFF method gives a relation that connects the rate of change of the target pose in end-effector frame to the rate of change of the joint angles. We use the relation to compensate the fictional motion of the target based on the

joint velocity, and extract the real motion of the target in the camera images, which can improve the performance of the image recognition unit, making the recognition system dynamically stable.

We use model-based method to recognize 3-D target's pose in real-time. The matching degree of the model to the target can be estimated by a fitness function, whose maximum value represents the best matching and can be solved on-line by"1-Step GA" [4]. Unit quaternion is used to represent the orientation of the target object, which has an advantage that can represent the orientation of a rigid body without singularities.

The effectiveness of the hand & eye-vergence dual visual servoing is evaluated through simulations incorporated with actual dynamics of 7-DoF robot on the view points of how the new idea improved the stability in visual servoing dynamics and the accuracy of hand pose.

II. Trackbility of the visual servoing system

In the actual experiment sometimes the object moves so fast that the manipulator can not catch up the speed of it, then the object may disappear in the sight of the cameras, while the system will recognize a wrong object in this case the the manipulator may do some unexpectable actions and broke itself even hurt the people. So in visual servoing system it is very important to make the camera tracking the object, so we present a concept: trackability. It can evaluate the ability of a visual servoing system of tracking the object. A system with high trackbility also have better security and validity.

When the object moves quickly, because of the high weight of the manipulator, the system may not catch up with the object, if the camera lose the object, it is dangerous, To solve this problem we control the camera and manipulator seperately. Because of the low weight and moment inertia of the camera, it can track the object better.

III. Simulator and robot dynamics

The Mitsubishi PA-10 robot arm is a 7 DOF robot arm manufactured by Mitsubishi Heavy Industries. Our simulator is model PA-10 (see Fig. 1), by using the actual physical parameters of the PA-10.

The general equation of motion of manipulator is

$$\boldsymbol{M}(\boldsymbol{q})\ddot{\boldsymbol{q}} + \boldsymbol{h}(\boldsymbol{q},\dot{\boldsymbol{q}}) + \boldsymbol{g}(\boldsymbol{q}) + \boldsymbol{d}(\dot{\boldsymbol{q}}) = \boldsymbol{\tau}, \tag{1}$$

where, $\boldsymbol{q}$: the joint displacement and $\boldsymbol{q} = [q_1, q_2, \cdots, q_7]^T$, $\boldsymbol{\tau}$: the joint driving force and $\boldsymbol{\tau} = [\tau_1, \tau_2, \cdots, \tau_7]^T$, $\boldsymbol{M}(\boldsymbol{q})$: the inertia matrix, $\boldsymbol{h}(\boldsymbol{q},\dot{\boldsymbol{q}})$: the vector representing the centrifugal and coriolis forces, $\boldsymbol{g}(\boldsymbol{q})$: the vector representing the gravity load, $\boldsymbol{d}(\dot{\boldsymbol{q}})$: the vector representing the frictional force. Here, we assumed $\boldsymbol{d}(\dot{\boldsymbol{q}}) = \boldsymbol{0}$.

Two cameras are mounted on the end-effector, modeling CCD-TRV86 manufactured by Sony Industries. The frame frequency of stereo cameras is set as 33fps. The structure of the manipulator and the cameras are shown as To evaluate the trackability of a system, we should have the whole modle of the system first in the research before we always ignore the mass and moment inertia of the camera system. In this simulation we also consider the mass and moment inertia of the two cameras, for the two cameras are installed on the same link the dynamic problem is a little different to the former one.

IV. Motion-Feedforward (MFF) Compensation

A. Analysis of target's motion in Σ_E

The target coordinate system is represented as Σ_M. Since solid models used to search for the target object are located in the end-effector's coordinate Σ_E, here we discuss the changing of ${}^E\boldsymbol{\psi}_M$ based on the changing of ${}^W\boldsymbol{\psi}_M$ and the configuration of the robot determined by $\boldsymbol{q}$. Such a relation will be described by the following mathematical function, which can distinguish these two affected motions clearly.

$$\begin{aligned}
{}^E\dot{\boldsymbol{\psi}}_M &= \begin{bmatrix} {}^E\dot{\boldsymbol{r}}_M \\ {}^E\dot{\boldsymbol{\epsilon}}_M \end{bmatrix} \\
&= \begin{bmatrix} -{}^E\boldsymbol{R}_W(\boldsymbol{q})\boldsymbol{J}_p(\boldsymbol{q}) + {}^E\boldsymbol{R}_W(\boldsymbol{q}) \\ \boldsymbol{S}({}^W\boldsymbol{R}_E(\boldsymbol{q}){}^E\boldsymbol{r}_M)\boldsymbol{J}_o(\boldsymbol{q}) \\ -\frac{1}{2}({}^E\eta_M\boldsymbol{I} - \boldsymbol{S}({}^E\boldsymbol{\epsilon}_M)){}^E\boldsymbol{R}_W(\boldsymbol{q})\boldsymbol{J}_o(\boldsymbol{q}) \end{bmatrix} \dot{\boldsymbol{q}} \\
&\quad + \begin{bmatrix} {}^E\boldsymbol{R}_W(\boldsymbol{q}) & 0 \\ 0 & {}^E\boldsymbol{R}_W(\boldsymbol{q}) \end{bmatrix} \begin{bmatrix} {}^W\dot{\boldsymbol{r}}_M \\ {}^W\dot{\boldsymbol{\epsilon}}_M \end{bmatrix} \\
&= \boldsymbol{J}_M(\boldsymbol{q},{}^E\boldsymbol{\psi}_M)\dot{\boldsymbol{q}} + \boldsymbol{J}_N(\boldsymbol{q}){}^W\dot{\boldsymbol{\psi}}_M.
\end{aligned} \tag{2}$$

Please refer to [3] for a detailed deduction procedural of (2). The matrix $\boldsymbol{J}_M$ in (2) describes how target pose change in Σ_E with respect to changing manipulator pose in Σ_E. The matrix $\boldsymbol{J}_N$ in (2) describes how target pose change in Σ_E with respect to the pose changing of itself in real word.

In this paper, we do not deal with the prediction of the target's motion in the real world, we take account of the prediction of the target velocity in Σ_E based on the joint velocity $\dot{\boldsymbol{q}}$ of the manipulator, so we can rewrite (2) as

$${}^E\dot{\boldsymbol{\psi}}_M = \boldsymbol{J}_M(\boldsymbol{q},{}^E\boldsymbol{\psi}_M)\dot{\boldsymbol{q}}. \tag{3}$$

Then the 3-D pose of the target at time $t + \Delta t$ can be predicted based on the motion of the end-effector motion at time t, presented by

$${}^E\boldsymbol{\psi}_M(t+\Delta t) = {}^E\boldsymbol{\psi}_M(t) + {}^E\dot{\boldsymbol{\psi}}_M\Delta t. \tag{4}$$

B. MFF Compensation

In the same way as the above equation (3), (4), the pose of the individuals $\boldsymbol{\psi}_{i,j}$ in the next $j+1$ generation can be predicted based on the current pose,

$$\dot{\boldsymbol{\psi}} = \boldsymbol{J}_M(\boldsymbol{q},\hat{\boldsymbol{\psi}}(t))\dot{\boldsymbol{q}}. \tag{5}$$

$$\boldsymbol{\psi}_{i,j+1}(t+\Delta t) = \boldsymbol{\psi}_{i,j}(t) + \dot{\boldsymbol{\psi}}\Delta t, \tag{6}$$

where Δt is the time cost in one generation. By using (6), GA group will move together with the motion of the target in Σ_E, never loose it even under a high-speed moving of robot manipulator, Since the effect on the recognition from the dynamics of manipulator can be compensated, recognition by hand-eye cameras will be independent of the dynamics of the manipulator, robust recognition can be obtained just like using fixed cameras.

V. HAND & EYE VISUAL SERVOING

A. Desired-trajectory generation

End-effector's motion of the target object in Σ_W is described by Homogeneous Transformation as ${}^{W}\boldsymbol{T}_{M}(t)$, and the desired relative relationship of Σ_M and Σ_E is given by ${}^{Ed}\boldsymbol{T}_{M}(t)$, the a desired-trajectory of the robot's end-effecter is determined by

$$ {}^{W}\boldsymbol{T}_{Ed}(t) \quad = \quad {}^{W}\boldsymbol{T}_{M}(t){}^{Ed}\boldsymbol{T}_{M}^{-1}(t) \tag{7} $$

${}^{E}\boldsymbol{T}_{Ed}$ can be described by

$$ {}^{E}\boldsymbol{T}_{Ed} \quad = \quad {}^{E}\hat{\boldsymbol{T}}_{M}(\hat{\boldsymbol{\psi}}(t))\ {}^{M}\boldsymbol{T}_{Ed}(t), \tag{8} $$

Notice that Eq. (8) is a general deduction that satisfies arbitrary object motion ${}^{W}\boldsymbol{T}_{M}(t)$ and arbitrary objective of visual servoing ${}^{Ed}\boldsymbol{T}_{M}(t)$.

Differentiating Eq. (8) with respect to time yields

$$ {}^{E}\dot{\boldsymbol{T}}_{Ed}(t) = {}^{E}\dot{\hat{T}}_{M}(t){}^{M}\boldsymbol{T}_{Ed}(t) + {}^{E}\hat{\boldsymbol{T}}_{M}(t){}^{M}\dot{\boldsymbol{T}}_{Ed}(t), \tag{9} $$

Differentiating Eq. (9) with respect to time again

$$ {}^{E}\ddot{\boldsymbol{T}}_{Ed}(t) = {}^{E}\ddot{\hat{T}}_{M}(t){}^{M}\boldsymbol{T}_{Ed}(t) + 2{}^{E}\dot{\hat{T}}_{M}(t){}^{M}\dot{\boldsymbol{T}}_{Ed}(t) + {}^{E}\hat{\boldsymbol{T}}_{M}(t){}^{M}\ddot{\boldsymbol{T}}_{Ed}(t), \tag{10} $$

Where, ${}^{M}\boldsymbol{T}_{Ed}$, ${}^{M}\dot{\boldsymbol{T}}_{Ed}$, ${}^{M}\ddot{\boldsymbol{T}}_{Ed}$ are given as the desired visual servoing objective. ${}^{E}\hat{\boldsymbol{T}}_{M}$, ${}^{E}\dot{\hat{T}}_{M}$, ${}^{E}\ddot{\hat{T}}_{M}$ can be observed by cameras using the on-line evolutionary recognition method of 1-step GA.

B. Hand-Visual Servoing Controller

The block diagram of our proposed hand & eye visual servoing controller is shown in Fig. 1. The hand-visual servoing is the outer loop. The controller used for hand-visual servoing is proposed by B.Siciliano [5]. Here, we just show main equations of the controller to calculate $\boldsymbol{\tau}$, which is output to control the robot manipulator.

$$ \boldsymbol{a}_p = {}^{W}\ddot{\boldsymbol{r}}_{Ed} + \boldsymbol{K}_{D_p}{}^{W}\dot{\boldsymbol{r}}_{E,Ed} + \boldsymbol{K}_{P_r}{}^{W}\boldsymbol{r}_{E,Ed}, \tag{11} $$

$$ \boldsymbol{a}_o = {}^{W}\dot{\boldsymbol{\omega}}_{Ed} + \boldsymbol{K}_{D_o}{}^{W}\boldsymbol{\omega}_{E,Ed} + \boldsymbol{K}_{P_o}{}^{W}\boldsymbol{R}_{E}{}^{E}\Delta\boldsymbol{\epsilon}, \tag{12} $$

$$ \boldsymbol{\alpha}_1 = \boldsymbol{J}^{+}(\boldsymbol{q})\Big(\begin{bmatrix} \boldsymbol{a}_p \\ \boldsymbol{a}_o \end{bmatrix} - \dot{\boldsymbol{J}}(\boldsymbol{q},\dot{\boldsymbol{q}})\dot{\boldsymbol{q}}\Big) + \big(\boldsymbol{I} - \boldsymbol{J}^{+}(\boldsymbol{q})\boldsymbol{J}(\boldsymbol{q})\big) \big(\boldsymbol{E}_p(\boldsymbol{q}_0 - \boldsymbol{q}) + \boldsymbol{E}_d(\boldsymbol{0} - \dot{\boldsymbol{q}})\big), \tag{13} $$

Here, $\boldsymbol{\alpha}_1$ is a 7×1 vector, the error variables in (11), (12) are described in Σ_W , which can be obtained from the vectors in Σ_E in (8), (9), (10) using the rotational matrix ${}^{W}\boldsymbol{R}_{E}(\boldsymbol{q})$ through coordinate transformation.

And $\boldsymbol{J}^{+}(\boldsymbol{q})$ in (13) is the preudo-inverse of $\boldsymbol{J}(\boldsymbol{q})$ given by $\boldsymbol{J}^{+}(\boldsymbol{q}) = \boldsymbol{J}^{T}(\boldsymbol{J}\boldsymbol{J}^{T})^{-1}$.

It has been proved in [5] that the system is exponentially stable for any choice of positive definite $\boldsymbol{K}_{D_p}, \boldsymbol{K}_{D_o}$ and $\boldsymbol{K}_{P_p}, \boldsymbol{K}_{P_o}$, thus

$$ \lim_{t\to\infty}{}^{W}\boldsymbol{r}_{E,Ed} = \boldsymbol{0} \qquad \lim_{t\to\infty}{}^{W}\dot{\boldsymbol{r}}_{E,Ed} = \boldsymbol{0} \tag{14} $$

$$ \lim_{t\to\infty}{}^{E}\Delta\boldsymbol{\epsilon} = \boldsymbol{0} \qquad \lim_{t\to\infty}{}^{W}\boldsymbol{\omega}_{CR,CRd} = \boldsymbol{0}. \tag{15} $$

Then we have

$$ \lim_{t\to\infty}{}^{E}\boldsymbol{T}_{Ed} = \boldsymbol{I} \qquad \lim_{t\to\infty}{}^{E}\dot{\boldsymbol{T}}_{Ed} = \boldsymbol{0} \tag{16} $$

Substituting Eq. (16) to Eq. (8), we have

$$ \lim_{t\to\infty}{}^{E}\boldsymbol{T}_{M} = \lim_{t\to\infty}{}^{Ed}\boldsymbol{T}_{M} \tag{17} $$

Eq. (17) proves stable convergence of visual servoing.

The eye-vergence visual servoing is the inner loop of the visual servoing system shown in Fig. 1. In this paper, we use two pan-tilt cameras for eye-visual servoing. Here, the positions of cameras are supposed to be fixed. The left and right camera's poses are defined by $\boldsymbol{\phi}_L = [\psi, \theta_l]^T$, $\boldsymbol{\phi}_R = [\psi, \theta_r]^T$, where ψ is title angle θ_l and θ_r are pan angles, and that is common for both cameras. Another DoF for the pose of the cameras is the angle rotating around the z axis of Σ_E, which is the gazing direction of the camera. Our eye-vergence visual servoing system does not include this DoF because the gazing derection of the camera is not changing in this case, which is meaningless for improving target observability.

Since the object's measurement result $\hat{\boldsymbol{\psi}}$ is described in Σ_E, it can be transformed to Σ_{CL} and Σ_{CR} by Homogeneous Transformations as,

$$ {}^{CL}\hat{\boldsymbol{T}}_{M}({}^{CL}\hat{\boldsymbol{\psi}}(t)) = {}^{CL}\boldsymbol{T}_{E}(\boldsymbol{\phi}_L){}^{E}\hat{\boldsymbol{T}}_{M}(\hat{\boldsymbol{\psi}}(t)), \tag{18} $$

$$ {}^{CR}\hat{\boldsymbol{T}}_{M}({}^{CR}\hat{\boldsymbol{\psi}}(t)) = {}^{CR}\boldsymbol{T}_{E}(\boldsymbol{\phi}_R){}^{E}\hat{\boldsymbol{T}}_{M}(\hat{\boldsymbol{\psi}}(t)). \tag{19} $$

We set the desired poses of the cameras to satisfy that the cameras are both direct to the object.With the position and orientation of the object and the end-effector we can calculate the desired pose of the cameras ψ_d,θ_{Rd} and θ_{Ld}

$$ \boldsymbol{\alpha}_2 = \boldsymbol{K}_p(\boldsymbol{\phi}_d - \boldsymbol{\phi}) + \boldsymbol{K}_d(\dot{\boldsymbol{\phi}}_d - \dot{\boldsymbol{\phi}}) \tag{20} $$

where $\boldsymbol{K}_p$, $\boldsymbol{K}_d$ are positive control gain, $\boldsymbol{\alpha}$ is a 3×1 vector, and $\boldsymbol{\phi}$ is the vector of the tilt angle and the pan angles of the two cameras.

$$ \boldsymbol{\alpha} = \begin{bmatrix} \boldsymbol{\alpha}_1 \\ \boldsymbol{\alpha}_2 \end{bmatrix} \tag{21} $$

$$ \boldsymbol{\tau} = \boldsymbol{M}(\boldsymbol{q})\boldsymbol{\alpha} + \boldsymbol{h}(\boldsymbol{q},\dot{\boldsymbol{q}})\dot{\boldsymbol{q}} + \boldsymbol{g}(\boldsymbol{q}). \tag{22} $$

Here, $\boldsymbol{\alpha}$ and $\boldsymbol{\tau}$ are both 10×1 vectors, and $\boldsymbol{\tau}$ means the input torque of each joint.

VI. SIMULATION OF HAND & VISUAL SERVOING

To verify the effectiveness of the proposed hand & eye visual servoing system, we conduct the simulation of visual servoing to a 3D marker that is composed of a red ball, a green ball and a blue ball.

A. simulation condition

To check the trackbility of a system we will move the object in the experiment, The initial hand pose is defined as Σ_{E_0}, and the homogeneous transformation matrix from Σ_{E_0} to Σ_W is

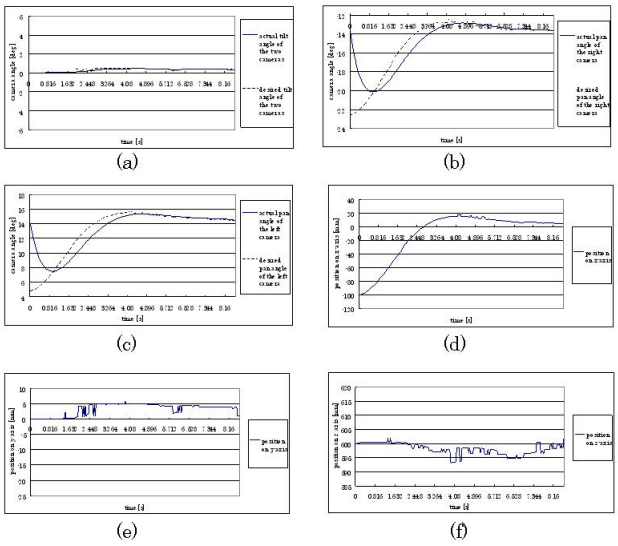

Fig. 2. Results of object in Σ_E and angle of the cameras

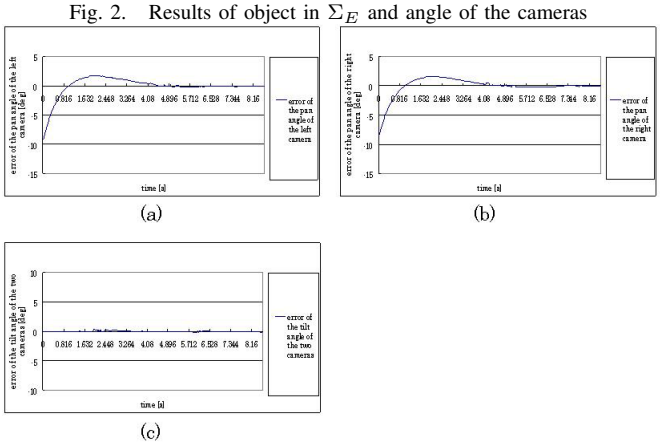

Fig. 3. Results of the difference between the actual and desired angles of the cameras

$$ {}^{W}\boldsymbol{T}_{E_0} = \begin{bmatrix} 0 & 0 & 1 & 918[mm] \\ -1 & 0 & 0 & 0[mm] \\ 0 & -1 & 0 & 455[mm] \\ 0 & 0 & 0 & 1 \end{bmatrix}. \quad (23) $$

While the initial object pose is defined as Σ_{M_0}, and the homogeneous transformation matrix from Σ_W to Σ_{M_0} is

$$ {}^{W}\boldsymbol{T}_{M} = \begin{bmatrix} 0 & 0 & 1 & 1518[mm] \\ -1 & 0 & 0 & 0[mm] \\ 0 & -1 & 0 & 455[mm] \\ 0 & 0 & 0 & 1 \end{bmatrix}. \quad (24) $$

We make the object move 100[mm] on the minus direction of X-axis of Σ_{M_0} at second 0, and keep the end-effector static to the object it recognized as (25).

$$ \begin{cases} {}^{M}x_{Ed}(t) = 0 \\ {}^{M}y_{Ed}(t) = 0 \\ {}^{M}z_{Ed}(t) = -600[mm] \\ {}^{M}\epsilon_{1Ed}(t) = 0 \\ {}^{M}\epsilon_{2Ed}(t) = 0 \\ {}^{M}\epsilon_{3Ed}(t) = 0 \end{cases} \quad (25) $$

B. simulation Results

Firstly, we analyze the data of the cameras and the position of the object expressed in the end-effector coordinate. Fig. 2 shows the results of object in Σ_E and angles of the cameras Fig. 2 (a) is the actual and desired tilt angles of the two cameras, while Fig. 2 (b) and (c) are the actual and desired pan angles of the right and the left camera. Here the desired angles are calculated out by the position of the recognized object express in the end-effector coordinate. Fig. 2 (c),(d),(e) are the recognized object expressed in the coordinate of the end-effector. For the step motion of the object is on x-axis in Σ_{E_0}, the change of the desired tilt angle is not very obvious. In Fig. 2 (b) and (c), when the object jump to (-100[mm],0[mm],600[mm]) in Σ_{E_0} on second 0, the desired angle also changed immediately accord to the motion of the object, while the actual angles also go forward the desired ones, in the two figures we can see the actual angle can catch the desired one on about 0.8 second. For the desired position of the end-effector is set as Fig. 25 about the object. We can know that the desired position of the object expressed in the coordinate of the end-effector is (0[mm],0[mm],600[mm]), In Fig. 2 (d) because of the step motion of the object is 100[mm] on the minus direction of x-axis in coordinate of the end-effector, the original value is -100[mm], and it reached the desired position on about 2.8 second. Compared with the data of the angles we can see the cameras can reach the desired value faster. Then, in Fig. 3 it shows the difference between the actual angles and the desired ones, it reflect the trackability of the system. We can see that the actual angles can reach the desired ones much faster than the convergence of the position of the end-effector in Fig. 3.

VII. Conclusion

In this paper, we put forward a new concept to evaluate the ability of tracking an object of a system, and introduce the importance of it. To check the trackability we found a whole model of PA-10 including the cameras' mass and moment inertia, The controller of the system includes two loops: an outer loop for conventional visual servoing that direct a manipulator toward a target object and an inner loop for active motion of binocular camera for accurate and broad observation of the target object. We compare the convergence speed of the end-effector and the angles of the cameras and evaluate the affection of trackbility of eye-vergence.

References

[1] S.Hutchinson, G.Hager, and P.Corke, "A Tutorial on Visual Servo Control", IEEE Trans. on Robotics and Automation, vol. 12, no. 5, pp. 651-670, 1996.

[2] E.Malis, F.Chaumentte and S.Boudet, "2-1/2-D Visual Servoing", IEEE Trans. on Robotics and Automation, vol. 15, no. 2, pp. 238-250, 1999.

[3] W. Song, M. Minami, Y. Mae and S. Aoyagi, "On-line Evolutionary Head Pose Measurement by Feedforward Stereo Model Matching", IEEE Int. Conf. on Robotics and Automation (ICRA), pp.4394-4400, 2007.

[4] H. Suzuki, M. Minami, "Visual Servoing to catch fish Using Global/local GA Search", IEEE/ASME Transactions on Mechatronics, Vol.10, Issue 3, 352-357 (2005.6).

[5] B.Siciliano and L.Villani: *Robot Force Control*, ISBN 0-7923-7733-8.